Supplement of

Measurement report: On the contribution of long-distance transport to the secondary aerosol formation and aging

Haobin Zhong[1,2], Ru-Jin Huang[1,2,3], Chunshui Lin[1], Wei Xu[1], Jing Duan[1], Yifang Gu[1,2], Wei Huang[1], Haiyan Ni[1], Chongshu Zhu[1], Yan You[4], Yunfei Wu[5], Renjian Zhang[5], Jurgita Ovadnevaite[6], Darius Ceburnis[6], Colin D. O'Dowd[6]

[1]State Key Laboratory of Loess and Quaternary Geology (SKLLQG), Center for Excellence in Quaternary Science and Global Change, and Key Laboratory of Aerosol Chemistry and Physics, Institute of Earth Environment, Chinese Academy of Sciences, Xi'an 710061, China

[2]University of Chinese Academy of Sciences, Beijing 100049, China

[3]Open Studio for Oceanic-Continental Climate and Environment Changes, Pilot National Laboratory for Marine Science and Technology (Qingdao), 266061 Qingdao, China

[4]National Observation and Research Station of Coastal Ecological Environments in Macao, Macao Environmental Research Institute, Macau University of Science and Technology, Macao SAR 999078, China

[5]Key Laboratory of Middle Atmosphere and Global Environment Observation (LAGEO), Institute of Atmospheric Physics, Chinese Academy of Sciences, Beijing 100029, China

[6]School of Physics and Ryan Institute's Centre for Climate & Air Pollution Studies, National University of Ireland Galway, University Road, Galway H91CF50, Ireland

Correspondence to: Ru-Jin Huang (rujin.huang@ieecas.cn)

S1. OA source apportionment

Positive matrix factorization (PMF) was used to interpret the number of factors in OA spectrum. The optimal number was selected by the discrimination of the tracers and the spectrum pattern of each source.

HOA (hydrocarbon like OA) is characterized by alkyl fragment ion series, which are in the form of C_nH_{2n-1} and C_nH_{2n+1}, and has dominated ion tracers such as *m/z* 41, 43, 55, 57, 69, 71, 83 and 85 in the spectra.

COA is also characterized by prominent hydrocarbon ion series, however, with higher signal at C_nH_{2n-1} than C_nH_{2n+1}. The higher signal ratio of $C_4H_7^+/C_4H_9^+$ is the typical characteristic of COA profile according to the previous studies (Ng et al., 2011).

Free PMF runs from 2 to 8 factors were performed in this study. When N=4, two POAs and two OOAs were separated, which were more reasonable than the results of the other numbers of factors. However, HOA was slightly mixed with COA in the PMF results, therefore, we further constrained HOA by using HOA profiles in ME-2 for clearer profiles.

HOA was constrained by using the profile from Ng et al. (2011), which was the average of 15 sites in the world including East Asia, Europe and North America. Previous study has discussed the HOA profile from US (dominated by gasoline) and Europe (dominated by diesel) through the means of cosine similarity analyses, and suggested that HOA profile from different types of cars were nearly equivalent (Elser et al., 2016).

We performed *a* value of HOA which was ranged from 0 to 1 with a step of 0.1 based on the results of 4 factors PMF solutions. After HOA was constrained, the other unconstrained factors show good consistency with previously reported profiles when the *a* value ranged from 0 to 0.8. To optimize the results, 9 solutions from 11 *a* value results were retained through the similar pattern with previously reported profiles, and the average of these 9 solutions were retained as final result (Figure S4).

The final OA source apportionment results were presented in figure S4. HOA was correlated with BC (R^2=0.48) and COA was well correlated with $C_6H_{10}O^+$ (R^2=0.81). Meanwhile, OOA was highly correlated with the oxygenated ions, which MO-OOA was highly correlated with CO_2^+ (R^2=0.89) and LO-OOA was highly correlated with $C_2H_3O^+$ (R^2=0.93). MO-OOA was the dominant pollutant in our result (55% or 3.7 μg m^{-3}), followed by LO-OOA (23% or 1.6 μg m^{-3}), COA (15% or 1.0 μg m^{-3}) and HOA (7% or 0.5 μg m^{-3}). The time series of OOA, COA and HOA correlated well with the corresponding tracers and precursors.

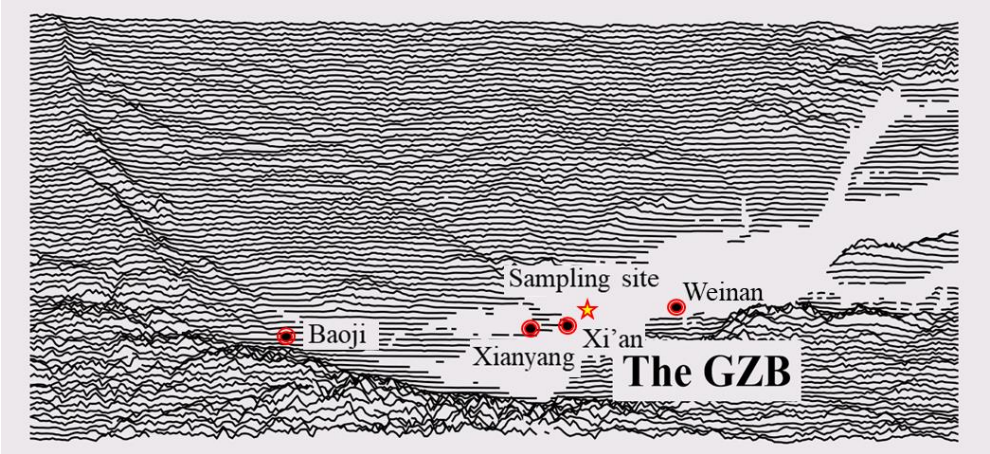

Figure S1. The schematic diagram of the topography of the GZB.

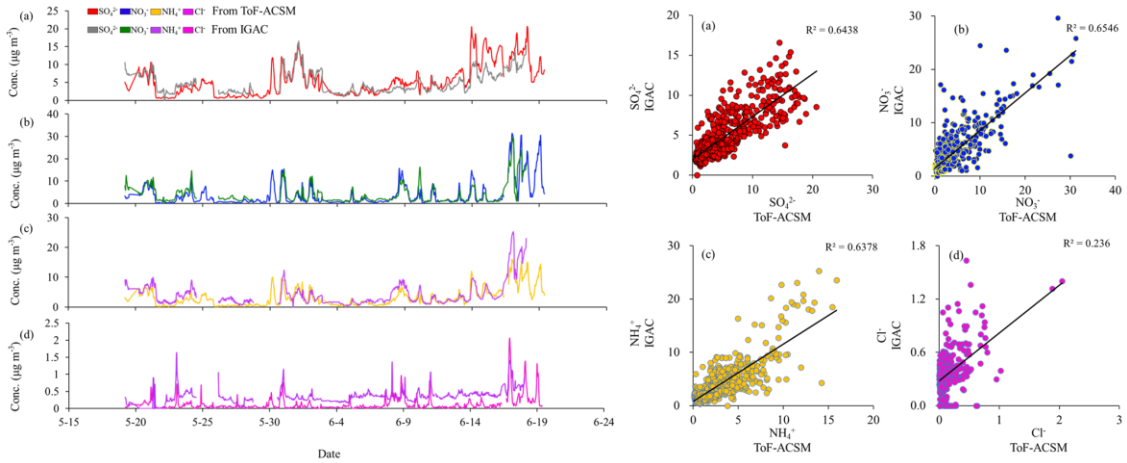

Figure S2. Time series and relationship of sulphate, nitrate, ammonium and chloride from

TOF-ACSM v.s. water soluble sulphate, nitrate, ammonium and chloride from IGAC.

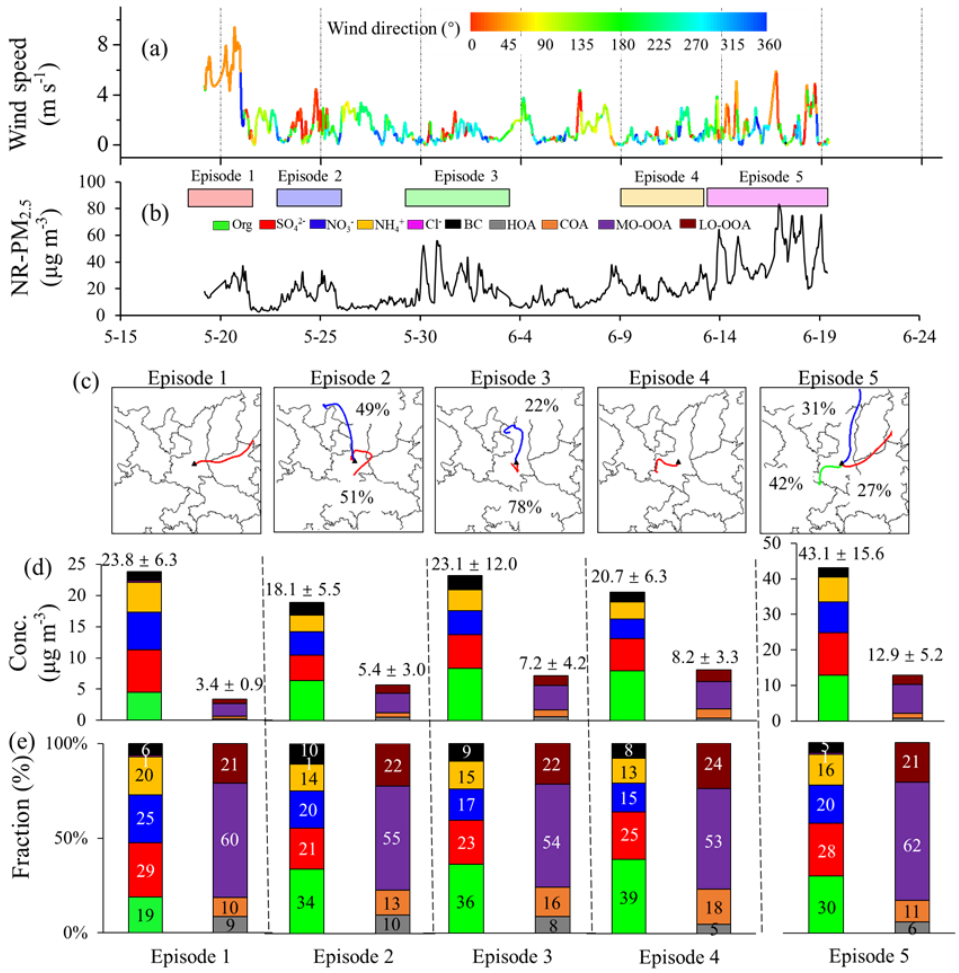

Figure S3. Five pollution episodes (EP1-EP5) and their corresponding (a) time series of wind speed and wind direction, (b) time series of $PM_{2.5}$ mass, (c) backward trajectories, (d) mass concentrations of chemical compositions (left column) and OA factors (right column) and (e) percentage contribution of chemical compositions (left column) and OA factors (right column). EP1 and EP4 are the only two pollution episodes caused by continuous transport from the BTH transport and the urban GZB transport respectively and are further discussed in the main text of the manuscript. Therefore, they are renamed as EP1 and EP2 respectively in the main text to lessen confusion.

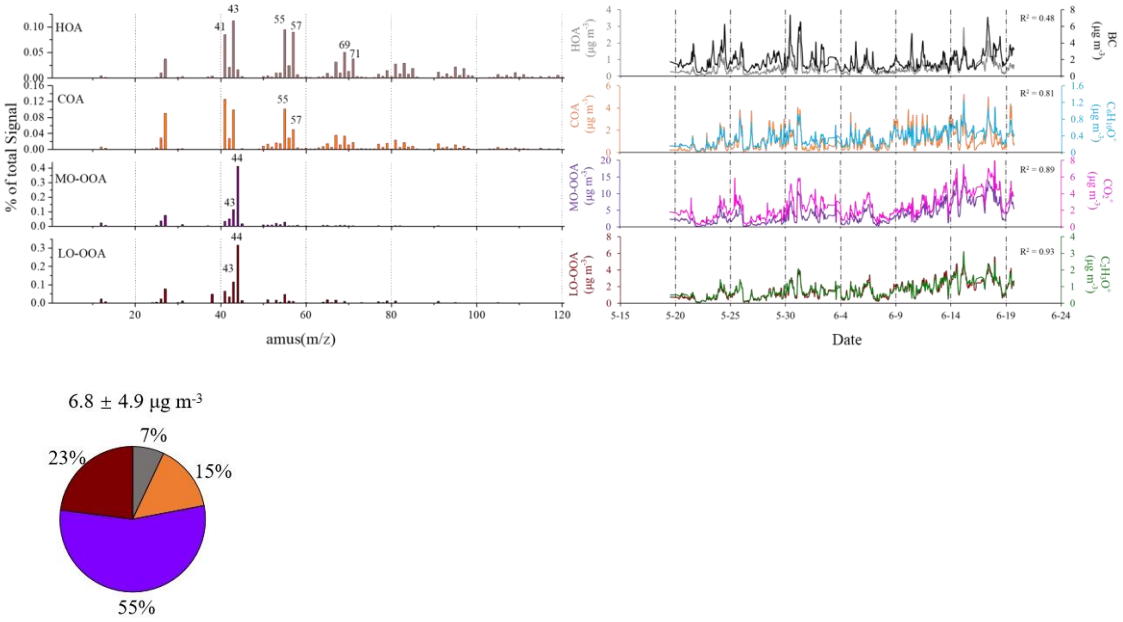

Figure S4. Profiles and time series of four OA factors. The external trace species, including BC, $C_6H_{10}O^+$, CO_2^+, $C_2H_3O^+$ are also shown for comparison.

Reference

Elser, M., Huang, R.-J., Wolf, R., Slowik, J.G., Wang, Q., Canonaco, F., Li, G., Bozzetti, C., Daellenbach, K.R., Huang, Y., Zhang, R., Li, Z., Cao, J., Baltensperger, U., ElHaddad, I., Prevot, A.S.H.: New insights into PM2.5 chemical composition and sources in two major cities in China during extreme haze events using aerosol mass spectrometry. Atmos. Chem. Phys. 16, 3207–3225, 2016.

Ng, N. L., Canagaratna, M. R., Jimenez, J. L., Zhang, Q., Ulbrich, I. M., and Worsnop, D. R.: Real-time methods for estimating organic component mass concentrations from aerosol mass spectrometer data, Environ. Sci. Technol., 45, 910–916, 2011.